Efficiency Enhancement in a Tapered Free Electron Laser by Varying the Electron Beam Radius

Y. Jiao[1], J. Wu[1], Y. Cai[1], A.W. Chao[1], W.M. Fawley[1], J. Frisch[1], Z. Huang[1], H.-D. Nuhn[1], C. Pellegrini[1,2], S. Reiche[3]

[1]*SLAC National Accelerator Laboratory, Menlo Park, CA 94025, USA*

[2]*Department of Physics and Astronomy, UCLA, Los Angeles, CA 90095-1547, USA*

[3]*Paul Scherrer Institute, Villigen PSI, 5232, Switzerland*

Abstract Energy extraction efficiency of a free electron laser (FEL) can be increased when the undulator is tapered after the FEL saturation. By use of ray equation approximation to combine the one-dimensional FEL theory and optical guiding approach, an explicit physical model is built to provide insight to the mechanism of the electron-radiation coherent interaction with variable undulator parameters as well as electron beam radius. The contribution of variation in electron beam radius and related transverse effects are studied based on the presented model and numerical simulation. Taking a recent studied terawatt, 120 m long tapered FEL as an example, we demonstrate that a reasonably varied, instead of a constant, electron beam radius along the undulator helps to improve the optical guiding and thus the radiation output.

I.INTRODUCTION

The latest scientific research requirements, like coherent diffraction imaging of complex molecules such as proteins, stimulate the efforts worldwide (in DESY [1] and SLAC [2]) to push the radiation power of a hard X-ray FEL with a tapered undulator to terawatt (TW) level, with a factor of 50 times increment compared to that of the self-amplified spontaneous emission (SASE) mode at saturation with similar electron beam parameters but a constant parameter undulator. It requires an in-depth understanding of the tapering-related physics so as to explore the full potential of a tapered FEL, not only by tapering the undulator parameters in longitudinal dimension, but also optimizing the transverse effects. Based on the one-dimensional (1D) FEL theory and the optical guiding approach [3-7], we build a physical model for the coherent electron-radiation interaction in a tapered FEL. With both the proposed physical model and numerical simulation, it is found that a reasonable variation of electron beam radius (or the transverse focusing) along the undulator can enhance the electron-radiation interaction and improve the radiation output as compared to the case of constant electron beam radius.

In Ref. [3], Kroll, Morton, and Rosenbluth (KMR) derived the equations that describe the electrons' synchrotron oscillations in the "bucket" associated with the ponderomotive potential in terms of the wiggler magnetic field, wiggler period and radiation field, using the Hamiltonian approach. They used the "bucket" parameters, i.e. the synchronous phase Ψ_r and bucket height $\delta\gamma_{\text{bucket}}/\gamma$, to express the electron trapping fraction F_t, and obtained an explicit formulation. However, the transverse effects are greatly simplified in their deviation by the assumption of constant radiation spot size r_s and electron beam radius r_b, and transverse uniform distribution of the radiation field and electron density.

In Ref. [5, 6], it is shown that the coherent interaction between the radiation and electrons can optically guide and focus the light. Because of its microbunching, the electron beam has an effective complex index of refraction n greater than unity,

$$n = 1 + \frac{\omega_{p0}^2}{\omega_s^2}\frac{r_{b0}^2}{r_b^2}\frac{a_w}{2|a_s|}F_t[JJ] < \frac{e^{-i\Psi}}{\gamma} >, \qquad (1)$$

Work supported in part by US Department of Energy contract DE-AC02-76SF00515.

where ω_p is the electron plasma frequency, $\omega_s = k_s c = 2\pi c/\lambda_r$ is the radiation frequency, with λ_r the radiation wavelength and c the speed of light, r_b is the electron beam radius, $a_w = |e|B_w/k_w mc^2$ and $a_s = |e|A_s/mc^2$ are the normalized vector potentials of the helical undulator and on-axis radiation fields (an additional $2^{1/2}$ factor in denominator for the linearly polarized undulator), with e the elementary charge, mc^2 the rest mass energy of electron, B_w the undulator field amplitude and $\lambda_w = 2\pi/k_w$ the undulator period, [JJ] is the Bessel function difference coupling term, γ is the electron's Lorentz factor, Ψ is the electron phase relative to the ponderomotive potential, and quantities with subscript 0 indicate the initial radiation and electron beam parameters. After the exponential growth region in a tapered FEL, the imaginary part of n, Im(n) which indicates the gain, is generally close to 0, and the real part Re(n), describing the refractive guiding dominates. It is noted [7, 8] that in this region $|a_s|$ increases much less rapidly than that in the previous exponential growth region, along with increase in the radiation spot size r_s. The continuously decreasing refractive guiding causes slowing down or even stopping of the $|a_s|$ growth. The optical guiding approach (especially Sprangle, Ting, and Tang's work [6]) includes the transverse effects self consistently. However, as shown in Eq. (1), the term $\langle \exp(-i\Psi) \rangle$ is obtained by averaging over all electrons, which naturally calls for numerical simulation with a large number of microparticles, rather than theoretical analysis, to study the physics in a tapered FEL.

In Sec. II, with ray equation approximation, we include the transverse effects revealed by the optical guiding approach in the frame of KMR's 1D FEL theory. In our model, both the radiation field and electron density depend on the transverse coordinate r, while following KMR the ponderomotive motions of electrons with the same r are characterized by the synchronous phase Ψ_r. As a result, the term $\langle \exp(-i\Psi) \rangle$ is calculated by averaging $\exp(-i\Psi_r)$ over r, instead of averaging over all electrons, resulting in more explicit and easier-to-handle formulation than the traditional optical guiding approach. Similar treatments are done for the electron trapping fraction F_t. In Sec. III, we compare the predictions of the proposed model with the GENESIS [9] time-steady simulation results. The agreement is very good. Moreover, in Sec. IV, we use this model to analyze the effects of a varied, instead of a constant, electron beam radius (periodic transverse focusing) in a tapered FEL, and take a TW, 120 m long FEL for illustration. It shows the energy extraction efficiency and the radiation output can be enhanced by a reasonable variation of electron beam radius (transverse focusing).

II. PHYSICAL MODEL FOR A TAPERED FEL

Generally, fundamental transverse Gaussian mode dominates the radiation along the undulator in a tapered FEL. Thus in our model only fundamental mode is considered. The normalized vector potential of the radiation field a_s is

$$a_s(r,z) = a_{s0}(z) e^{i\phi(r,z)} e^{\frac{-r^2}{r_s^2(z)}}, \tag{2}$$

where a_{s0} is the on-axis amplitude and ϕ is the phase of the radiation field. And accordingly, the radiation power P is given by

$$P(z) = \frac{\pi r_s^2(z) a_{s0}^2}{4Z_0} \left(\frac{k_s mc^2}{e}\right)^2, \tag{3}$$

with $Z_0 \approx 376.7\ \Omega$ being the impedance of free space.

From energy conservation, the change of $a_{s0}(z)$ from longitudinal position z_1 to z_2 can be evaluated by

$$a_{s0}^2(z_2)r_s^2(z_2)-a_{s0}^2(z_1)r_s^2(z_1)=\frac{\omega_{p0}^2}{\omega_s^2}r_{b0}^2F_t(z_1)(<\gamma(z_1)>-<\gamma(z_2)>), \qquad (4)$$

where it is assumed the variation of F_t is much slower than that of a_{s0}.

Under approximations such as the radiation beam remains approximately Gaussian and the betatron oscilation of the beam electrons is negligible on the time scale of the synchrotron oscillation, the evolution of the radiation spot size r_s follows the envelop equation [7],

$$r_s''+K^2r_s=0, \qquad (5)$$

where the optical focusing term K^2 can be written in terms of the refractive guiding "fiber parameter" V^2 with on-axis $|a_s|$, the average of sine and cosine of Ψ, and the filling factor $G(z) =(1-f)/(1+f)^2$ with $f(z) = (r_b/r_s)^2$,

$$K^2=\frac{4}{k_s^2}(-1+V^2G+\frac{1}{4}V^4G^2\frac{<\sin\Psi>^2}{<\cos\Psi>^2}+\frac{1}{4}k_sr_s^2\frac{d(V^2G/<\cos\Psi>)}{dz}<\sin\Psi>)r_s^{-4}. \qquad (6)$$

Because refractive guiding dominates after the initial saturation, Re(n) ≈ 1 and Im(n) << 1, the "fiber parameter" V^2 can be written as [5]

$$V^2(z)=(n^2-1)k_s^2r_b^2\approx 2[\mathrm{Re}(n)-1]k_s^2r_b^2=\frac{\omega_{p0}^2r_{b0}^2}{c^2}\frac{a_w}{a_{s0}}F_t[JJ]<\frac{\cos\Psi}{\gamma}>. \qquad (7)$$

We now consider the electrons' ponderomotive motion with taper. The electrons trapped into the "bucket" have their energies following the resonant condition [3],

$$\gamma_r^{\ 2}(z)=\frac{k_s}{2k_w(z)}(1+a_w^2(z)). \qquad (8)$$

To keep the analysis tractable, we assume the beam electrons are monoenergetic and replace $<\gamma(z)>$ in Eqs. (4, 7) by $\gamma_r(z)$.

Following the definition of the synchronous ponderomotive phase Ψ_r in Ref. [3], we have

$$\Psi_r=\sin^{-1}(\frac{-\gamma_r(z)\gamma_r'(z)}{a_w(z)k_s|a_s|}). \qquad (9)$$

From Eq. (2), $|a_s|$ varies with transverse coordinate r, thus Ψ_r depends on r. In general $\gamma_r' < 0$ and $\Psi_r(r, z) > 0$ in a tapered FEL.

For a specific positive Ψ_r, only electrons of energy γ_r and phase Ψ satisfying

$$\Psi_1<\Psi<\Psi_2, \qquad (10)$$

will be trapped in the ponderomoitve "bucket", where Ψ_1 and Ψ_2 are minimum and maximum Ψ of the "bucket" boundary,

$$\Psi_2(r,z)=\pi-\Psi_r(r,z),$$

$$\cos\Psi_1(r,z)+\Psi_1(r,z)\sin\Psi_r(r,z)=\cos\Psi_2(r,z)+\Psi_2(r,z)\sin\Psi_r(r,z). \qquad (11)$$

Thus the fraction of electrons trapped in the "bucket" is

$$F_t(r,z)=\frac{\Psi_2(r,z)-\Psi_1(r,z)}{2\pi}, \tag{12}$$

which is as well dependent on *r*.

The bucket height $\delta\gamma_{bucket}/\gamma$ indicates the available maximum σ_γ/γ of the trapped particles,

$$\frac{\delta\gamma_{bucket}}{\gamma}=\frac{2}{1+a_w^2}\sqrt{a_w\,|\,a_s\,|[\cos\Psi_r-(\frac{\pi}{2}-\Psi_r)\sin\Psi_r]}. \tag{13}$$

In the case that $\delta\gamma_{bucket}/\gamma$ is smaller than σ_γ/γ, the electron trapping fraction will be smaller.

From Eqs. (9-13), the electrons at larger *r* have greater Ψ_r and lower F_t. Physically, the coherent electron-radiation interaction and the corresponding ponderomotive potential are weak at large *r* due to weak radiation field, and accordingly, the electrons at larger *r* always detrap more rapidly than those at smaller *r*. Note that $F_t(r, z) = 0$ when $\Psi_r(r, z) = \pi/2$. It imposes a limitation for the available maximum *r* of the trapped electrons,

$$r_{\max}(z)=-r_s(z)\{\ln[\sin\Psi_r(r=0,z)]\}^{1/2}=-r_s(z)\{\ln[\frac{-\gamma(z)\gamma'(z)}{a_{s0}(z)a_w(z)k_s}]\}^{1/2}. \tag{14}$$

Assuming the initial electron beam distribution has a Gaussian profile, we have

$$f(r)=\frac{N_e}{\pi r_{b0}^2}e^{-\frac{r^2}{r_{b0}^2}}, \tag{15}$$

where $N_e = \int f(r)2\pi r dr$ is the initial electron population.

To be consistent with the above formulation, once again, we use the ray equation approximation, i.e., electrons' trajectories are straight lines when they pass through the undulator. Therefore the total electron trapped fraction can be obtained by averaging $F_t(r, z)$ over all *r* (Because there is no trapped particle beyond r_{max}, so one needs only to integrate *r* from 0 to r_{max}),

$$F_t(z)=\frac{1}{N_e}\int_0^{r_{\max}}F_t(r,z)\,f(r)2\pi r dr, \tag{16}$$

And similarly, $<\cos\Psi>$, $<\sin\Psi>$ are given by

$$<\cos\Psi_r>(z)=\frac{1}{N_e}\int_0^{r_{\max}}\cos\Psi_r(r,z)F_t(r,z)\,f(r)2\pi r dr, \tag{17}$$

$$<\sin\Psi_r>(z)=\frac{1}{N_e}\int_0^{r_{\max}}\sin\Psi_r(r,z)F_t(r,z)\,f(r)2\pi r dr. \tag{18}$$

Now we consider an undulator with taper starting from the saturation location. In the upstream exponential growth region the undulator parameters are constant, γ_r = constant = γ_0, $\gamma' = 0$ and $\Psi_r = 0$. After the initial saturation, electrons can continuously lose energy in the form of radiation by tapering the undulator parameters, $a_w(z)$ and/or $k_w(z)$, corresponding to a decelerating "bucket" with $\gamma_r' < 0$ and $\Psi_r > 0$. The evolution of Ψ_r from 0 to a positive value implies a phase matching region, where electrons self-bunch and match their phases to the ponderomotive potential right after the taper start-point. At saturation, $P_{sat} = \rho P_{beam}$, the

saturation length is estimated by [10]

$$L_{sat} = \frac{\lambda_w}{4\pi\sqrt{3}\rho}\ln(\frac{9P_{sat}}{P_{in}}), \tag{19}$$

with ρ being the FEL parameter and P_{in} the input radiation power. And the normalized vector potential of the radiation field $a_{s0,sat}$ in a helical undualtor can be evaluated by [8]

$$a_{s0,sat} = \frac{2(1+a_{w0}^2)\rho^2}{a_{w0}[JJ]}, \tag{20}$$

with the approximation that the radiation spot size equals to the r_{b0} that maximizes the saturation power (an additional $2^{1/2}$ factor in denominator for the linearly polarized undulator). Now one can estimate the values of γ_r, Ψ_r, a_{s0} and r_s at saturation only with the input electron and radiation beam parameters. For a given tapering of the undulator parameters let us say $a_w(z)$ and variation of electron beam radius $r_b(z)$, starting from the saturation location, Eqs. (2-18) can be integrated to yield the evolution of (a_{s0}, r_s, Ψ_r and F_t) along the undulator system, without resorting to any numerical simulation code.

It is worth mentioning that the presented model is based on ray equation approximation rather than being derived strictly from the Maxwell equation. It well descries the evolution of the radiation field within r_{max} given by Eq. (13), which is more or less $3r_{b0}$, while not considering the radiation propagating outside this region. Moreover, the ray equation approximation implies the model applies only for the tapered FEL with betatron oscilation of the beam electrons slow compared with the synchrotron oscillation of trapped electrons.

III. VERIFICATION OF THE PHYSICAL MODEL

The proposed model is verified by comparing with the numerical simulations of the GENESIS code [10] for a TW, hard X-ray FEL with L_w = 120 m tapered and linearly polarized undulator. The input electron and radiation beam parameters are listed in Table I. With a preset quadratic undulator parameter tapering, scanning the taper ratio $\xi = 1-a_w(L_w)/a_w(z_0)$ and beam radius r_b (constant through the undulator) by using of the GENESIS time-steady simulation, results in a maximum power of 2.2 TW with $\xi = 0.12$ and constant beam radius r_b = 15 μm, as shown in Fig. 1. For this optimal case, we count the radiation power within $r = 3r_{b0}$, F_t as well as the on-axis $|a_s|$ and r_s by fitting a Gaussian to the radiation field data, and plot them in Fig. 2 as black solid lines. The radiation reaches saturation at z ≈ 20 m, with $a_{s0,sat} \approx 5.1\times10^{-6}$. The short length (~ 7 m) right after saturation is the phase matching region, along with high trapping fraction but slow growth in on-axis $|a_s|$. Subsequently, a fraction of electrons are trapped in the ponderomotive "bucket" and continuously lose energy in the form of radiation of wavelength λ_r, resulting in further increasing in $|a_s|$ which, at the same time, leads to a decrease in refractive guiding, and in turn, causes an increase in r_s and slows down the $|a_s|$ growth. From Eq. (9), a less rapid increasing $|a_s|$ produces an increased Ψ_r and reduced r_{max} for trapped electrons, and thus a decrease in the electron trapping fraction. When the "fiber parameter" V^2 falls to about 1 [5, 8], on-axis $|a_s|$ reaches its maximum value, and then decreases due to the weakened optical guiding. In addition, it is found that the energy spread of the trapped electron, σ_γ/γ, remains more or less ρ, 0.0011, which is much less than the relative reduction ratio of the resonant energy $\gamma_r \approx 0.1$. Thus the assumption of monoenergetic beam electrons is a good approximation for the realistic

circumstance in such a long tapered FEL. The transverse betatron oscillation period in z, $L_\beta \approx \pi\gamma r_b^2/\varepsilon_{x,n} \approx 60$ m, five times the synchrotron oscillation period [3] $L_s \approx \lambda_w[(1+a_w^2)/|a_{s0}|/a_w]^{1/2}/2 \approx$ 12 m. The ray equation approximation is approximately satisfied.

TABLE I. Main parameters for a TW, 120 m long FEL with tapered and linearly polarized undulator

Parameters	**Value**	**Unit**
Energy	13.64	GeV
Current	4000	Ampere
Normalized emittances $\varepsilon_{x,n}/\ \varepsilon_{y,n}$	0.3/0.3	μm-rad
E-beam pulse length (FWHM)	10	fs
Normalized undulator parameter a_{w0}	2.3832	
Undulator period λ_w	3.2	cm
Radiation wavelength λ_r	1.5	Angstrom
Peak radiation input power	5	MW

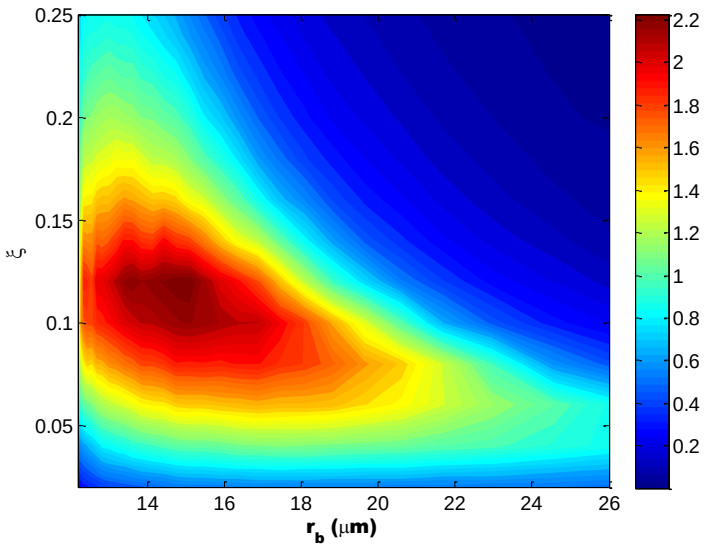

Fig. 1. Contour plot of radiation power with respect to taper ratio $\xi = 1-a_w(L_w)/a_w(z_0)$ and beam radius r_b, obtained by GENESIS time-steady simulations. The taper starts around the initial saturation point.

We have $L_{sat} = 16.1$ m and $a_{s0,sat} \approx 6.4\times10^{-6}$ from Eqs. (19, 20), and $\gamma_r = \gamma_0$, $\Psi_r = 0$, $r_s = r_{b0}$ and $F_t = 1$ by assuming the taper starts from the initial saturation point. With these parameters, the iterations of Eqs. (2-18) with step of 3.2 cm (while keeping constant $\Psi_r = 0$ and $F_t = 1$ in first two Rayleigh lengths right after the initial saturation to represent the phase matching region) qualitatively reproduce the GENESIS time-steady simulation results (see dashed lines in Fig. 2).

The success of the proposed model is also reflected in the transverse distribution of the electron beam and radiation field. As shown in Fig. 3, the transverse variation of the average

ponderomotive phase $\langle\Psi\rangle = \langle\theta + \phi\rangle$ (θ is the electron phase relative to a plane wave) obtained by the GENESIS time-steady simulation, shows the same tendency as that revealed by the physical model, i.e. electrons at larger r have greater Ψ_r.

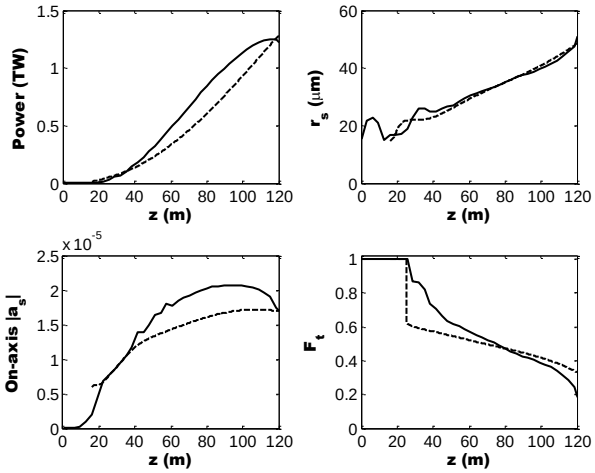

Fig. 2. Radiation power within $r = 3r_{b0}$ (top left), r_s (top right) and on-axis $|a_s|$ (bottom left) by fitting a Gaussian to the radiation field data and F_t (bottom right) along the undulator, obtained by GENESIS time-steady simulation (solid lines) and the proposed physical model (dashed lines).

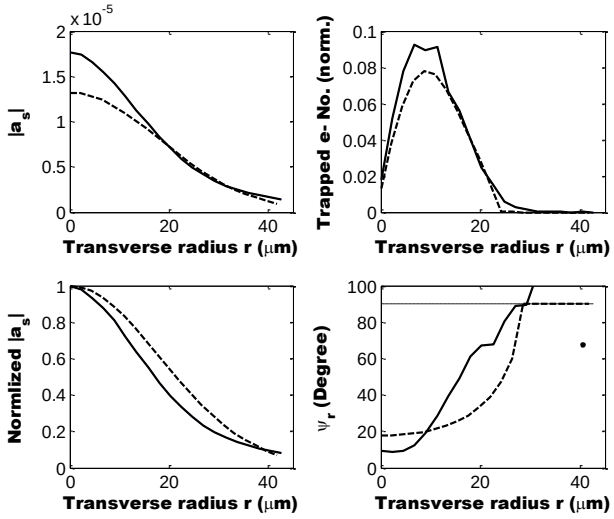

Fig. 3. Transverse distribution of $|a_s|$, normalized trapped electron number and Ψ at z = 50 m, obtained by GENESIS time-steady simulation (solid lines) and the proposed physical model (dashed lines).

IV. IMPROVING OPTICAL GUIDING WITH VARIED TRANSVERSE FOCUSING

In the exponential growth region, gain guiding minimizes diffraction effects and generally strong external focusing on the electron beam will minimize the gain length. However, in the tapered region well beyond initial saturation, gain guiding becomes much weaker and the radiation spot size starts to increase, it can require transverse focusing different from that in the exponential growth region. The presented model enables us to analyze the contribution of varying electron beam radius to the radiation output.

In the case of a gradually increased beam radius $r_b(z)$, the filling factor $G(z)$ and focusing

term $K^2(z)$ in Eqs. (5, 6) will be smaller, leading to larger radiation spot size $r_s(z)$ compared to the case of a constant r_b. The extracted energy from the electron beam is of a certain value, from Eq. (4), the on-axis $|a_s|$ will be smaller, causing larger on-axis Ψ_r and lower $F_t(r=0)$. So if it is decided to increase $r_b(z)$, the increment should be small enough to avoid significant detrapping. On the other hand, a larger $r_s(z)$ results in an increase in r_{max} (see Eq.(13)), yielding flatter transverse distribution of $|a_s|$ and Ψ_r. Electrons at large r will be trapped deeper inside the ponderomotive "bucket", which helps to avoid rapid detrapping for these electrons as subsequently the Ψ_r increases more rapidly associated with the slow-down in $|a_s|$ growth.

In contrast, squeezing $r_b(z)$ causes smaller $r_s(z)$ and r_{max}, as well as more rapid detrapping for the electrons at large r. However, it maintains high enough electron density neighboring the axis with dwindling trapped electrons' population and thus efficient optical guiding around axis, leading to more rapid growth in radiation on-axis $|a_s|$and less rapid increase in on-axis Ψ_r compared to the case of a constant r_b.

To test the contribution of a varied r_b, we start to decrease r_b from the 30 m location by linearly increasing quadupole strengths. Figs. 4 and 5 show the resulting on-axis $|a_s|$, r_s and F_t in comparison with the constant r_b case, obtained by the GENESIS time-steady simulation and the physical model, respectively. Both approaches predict higher on-axis $|a_s|$ and smaller r_s at the end of the undulator with a varied r_b.

Figure 6 shows the evolution of the total radiation power along the undulator for the cases with and without variation in r_b. With a varied r_b, GENESIS time-steady simulation predicts an increase in radiation power by a factor of 15%. When taking into account the time-dependent effects, the SASE components originating from shot noise on the electron beam can excite sideband instability in the tapered region [3, 11] and limit the available maximum radiation power. Even though, squeezing r_b in this case helps to produce more radiation power at the end of the undulator (2.16 vs. 1.96 TW) or reach the same radiation power within a shorter undulator length (92 vs. 95 m for 1.5 TW), compared to the case of a constant r_b.

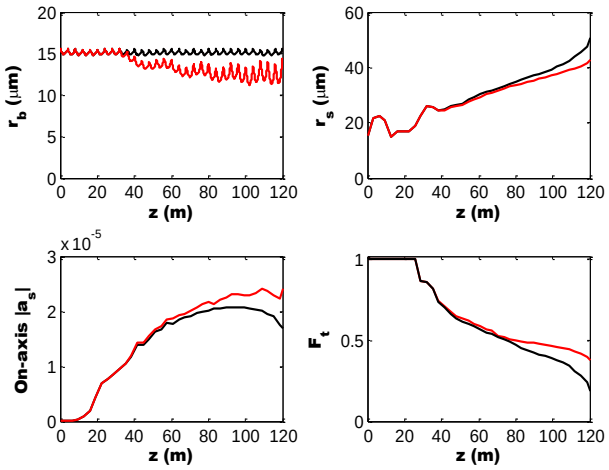

Fig. 4. On-axis $|a_s|$, r_s and F_t with constant (black lines) and varied (red lines) r_b, obtained by GENESIS time-steady simulation. The oscillation in r_b is due to imperfect optical matching.

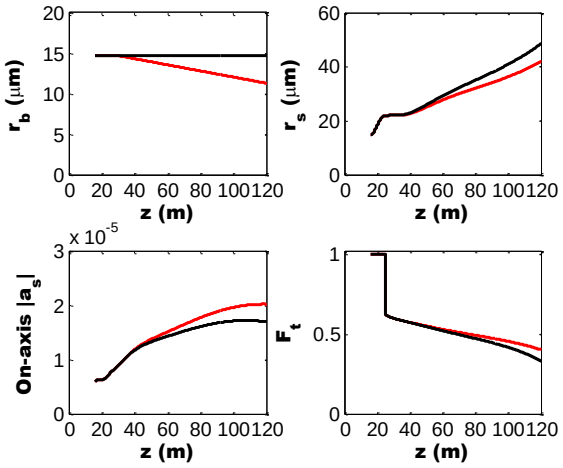

Fig. 5. On-axis $|a_s|$, r_s and F_t with constant (black lines) and varied (red lines) r_b, obtained by the proposed physical model.

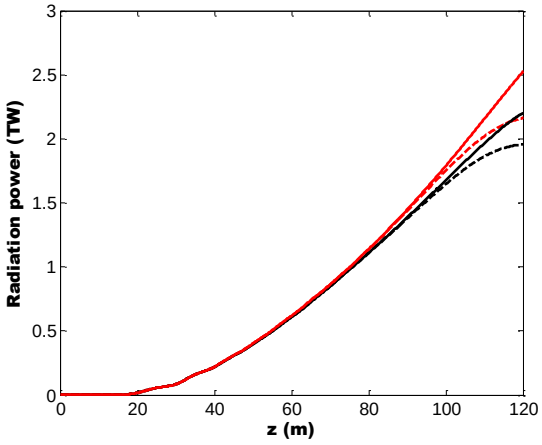

Fig. 6. GENESIS predictions for the radiation power evolution in a tapered, 120 m long undulator with (red lines) and without (black lines) variation in r_b for time-steady (solid lines) and full time-dependent conditions (dashed lines).

V. CONLUSION

By use of the ray equation approximation, we have built a physical model for the FEL physics in a tapered FEL, which has a remarkable success in predicting the behavior of the electron and radiation beam with variable undualtor parameters and varied electron beam radius (transverse focusing). Both the physical model and GENESIS numerical simulations show that a reasonable variation in the electron beam radius after the initial saturation can help to improve the optical guiding, electron trapping efficiency as well as the radiation output. In the TW FEL studied here for illustration, the radiation power increase is about 15%.

ACKNOWLEDGEMENTS

This work is supported by the Department of Energy under Contract No. DE-AC02-76SF00515.

Reference

[1] G. Geloni, V. Kocharyan, and E. Saldin, DESY 10-108, 2010.

[2] W.M. Fawley, J. Frisch, Z. Huang, Y. Jiao, H.-D. Nuhn, C. Pellegrini, S. Reiche, J. Wu, Proceedings of 2011 International Free Electron Laser Conference, Shanghai, China, 2011.

[3] N.M. Kroll, P.L. Morton and M.N. Rosenbluth, IEEE J. Quantum Electron. **17**, 1436 (1981).

[4] D. Prosnitz, A. Szoke and V.R. Neil, Phys. Rev. A **24**, 1436 (1981).

[5] E.T. Scharlemann, A.M. Sessler and J.S. Wurtele, Phys. Rev. Lett. **54**, 1925 (1985).

[6] P. Sprangle, A. Ting and C.M. Tang, Phys. Rev. Lett. **59**, 202 (1987).

[7] B. Hafizi, A. Ting, P. Sprangle and C.M. Tang, Phys. Rev. Lett. **64**, 180 (1990).

[8] W.M. Fawley, Nucl. Instrum. Methods Phys. Res., Section. A **375**, 550 (1996).

[9] S. Reiche, Nucl. Instrum. Methods Phys. Res., Section. A **429**, 243 (1999).

[10] M. Xie, Proceedings of 1995 Particle Accelerator Conference, Dallas, Texas, 1995, p. 183.

[11] Z. Huang and K.-J. Kim, Nucl. Instrum. Methods Phys. Res., Section. A **483**, 504 (2002).